

Research Article

SLC9A1 Binding mTOR Signaling Pathway-Derived Risk Score Predicting Survival and Immune in Clear Cell Renal Cell Carcinoma

Dengshuang Wu,^{1,2} Zhipeng Xu ^{1,3} and Jianning Wang ^{1,3}

¹Department of Urology, Shandong Provincial Qianfoshan Hospital, Cheeloo College of Medicine, Shandong University, Jinan, Shandong, China

²Department of Urology, Qingdao Municipal Hospital, Qingdao 266011, Shandong, China

³Department of Urology, The First Affiliated Hospital of Shandong First Medical University and Shandong Provincial Qianfoshan Hospital, Shandong Medicine and Health Key Laboratory of Organ Transplantation and Nephrosis, Shandong Institute of Nephrology, Jinan, China

Correspondence should be addressed to Zhipeng Xu; scofield_xzp@163.com and Jianning Wang; docjianningwang@163.com

Received 26 September 2022; Revised 18 October 2022; Accepted 27 January 2023; Published 13 February 2023

Academic Editor: Muhammad Muddassir Ali

Copyright © 2023 Dengshuang Wu et al. This is an open access article distributed under the Creative Commons Attribution License, which permits unrestricted use, distribution, and reproduction in any medium, provided the original work is properly cited.

Objective. Clear cell renal cell carcinoma (ccRCC) is one of the common renal cell carcinomas (RCC) with a high risk of recurrence. Considering that SLC9A1 is involved in various cellular physiological processes and probably mediates the course of mTOR signaling in tumors, this study constructed a risk model for SLC9A1 combined with mTOR signaling in ccRCC, aiming at better predicting the prognosis of patients. **Methods.** ccRCC expression matrices were downloaded from TCGA and ICGC databases to compare the expression of SLC9A1 in TCGA, and qRT-PCR was adopted to validate the SLC9A1 expression in different RCC cells and normal kidney cells. The CIBERSORT and ESTIMATE algorithms were used to assess samples for immunity. mTOR signaling-associated genes were downloaded from the KEGG website, and then the genes were adopted to screen genes associated with SLC9A1 expression and mTOR signaling pathway colleagues, based on which univariate COX regression and lasso regression Cox analyses were conducted to construct a ccRCC prognostic risk model. ROC curves and nomograms were used to assess the validity of the models. **Results.** ccRCC tumor samples showed lower SLC9A1 expression than normal samples, as also evidenced by qRT-PCR. The SLC9A1 expression was highly correlated with tumor immunity. Totally, 564 key genes associated with both SLC9A1 expression and mTOR signaling were screened out, and the risk model consisting of 11 gene signatures was constructed in ccRCC based on the 564 genes. Since patients at a high risk had poorer survival outcomes, the high-risk group presented poorer immunotherapy outcomes. Moreover, a higher clinical grade of patients suggested a higher risk score. The risk score can serve as one independent prognostic factor for the prognosis prediction of ccRCC patients. **Conclusion.** An extremely promising prognostic indicator for ccRCC based on SLC9A1 and mTOR signaling has been constructed to provide reference for clinical treatment.

1. Introduction

Renal cell carcinoma (RCC) is one of the most common solid tumors of the adult kidney [1]. Among its subtypes, clear cell renal cell carcinoma (ccRCC) is the major one, with a high rate of occurrence (accounting for 80–90% of all cases) and relapse risk [2, 3]. Moreover, about 30% of patients

presented distant metastasis during initial diagnosis [4]. Although the treatment of ccRCC has achieved great progress in recent years, especially immunotherapy, which has been considered an effective therapeutic method for advanced patients [5–7], cancer-specific morbidity and mortality continue to rise, and drug resistance persists unfortunately worldwide [8, 9]. The prognostic staging

system currently does not provide adequate guidance for treatment and cannot accurately predict clinical outcomes [10, 11]. Accordingly, it is urgent to identify the efficient prognostic model of ccRCC patients.

SLC9A1, also named Na/H exchanger 1 (NHE1) [12], belongs to the NHE exchanger family [13]. As a membrane protein, SLC9A1 exists in many mammalian cell types and is involved in intracellular pH (pHi) regulation [14, 15]. Many physiological processes are dependent on SLC9A1, including cell proliferation, cell volume regulation, cellular immunity, and cell death [16]. Furthermore, prior research has revealed that potential downstream impacts of mTOR on cell growth, survival, and tumorigenesis were under medication by SLC9A1 [17]. Reportedly, in gastric cancer, hepatocellular carcinoma (HCC), ovarian cancer, and gliomas, SLC9A1 favors tumorigenesis and predicts poor prognosis [13, 18, 19]. In breast cancer, SLC9A1 acts as a facilitator in tumor invasiveness [20]. Based on these findings, SLC9A1 protein has emerged as an important marker for tumorigenesis and prognosis, whereas the potential role of SLC9A1 in ccRCC has not been fully understood.

This study analyzed the SLC9A1 expression in ccRCC and its association with immunity. A prognostic risk model was established on the basis of SCL9A1 as well as mTOR signaling in ccRCC, with the purpose of finding possible prognostic markers in ccRCC and providing a theoretical basis for prognostic prediction of patients.

2. Materials and Methods

2.1. Cell Strains and Reagents. Human RCC cell strains (786-O, A498, OS-RC-2, ACHN, 769-P, Caki-1, and Caki-2) and human normal renal cells (293T and HK-2) were provided by American Type Culture Collection (ATCC, Rockville, MD, and the States). A498, ACHN, and HK-2 were incubated in MEM (Invitrogen, 11090-081). 786-O, 769-P, and OS-RC-2 were subjected to incubation in RPMI-1640 (Gibco, 11875500BT). Caki-1 and Caki-2 were subjected to incubation in Mccoy 5A (Gibco, 12330031). 293T was cultured in DMEM (Gibco, 11995500BT). The medium were supplemented with 10% fetal bovine serum (Gibco, the States). All the cell strains were maintained in an incubator (37°C, 5% CO₂).

2.2. RNA Isolation and Quantitative Real-Time PCR (qRT-PCR). Total RNA was extracted from cells through TRIzol reagent (Invitrogen). First-strand cDNA was generated from 1 µg total RNA using Hifair® II 1st Strand cDNA Synthesis Kit (11119ES60) from Yeasen (Shanghai, CN). qRT-PCR was conducted three times with a SYBR Green premix qPCR kit (Accurate Biotechnology, Changsha, Hunan, CN, AG11701). Sequences of primers for qRT-PCR were provided as follows: SLC9A: forward: 5'-ACCACGAGAACGCTCGATTG-3', reverse: 5'-ACGTGTGTGTAGTCGATGCC-3'. GAPDH: forward: 5'-GGAGCGAGATCCCTCCAA AAT-3', reverse: 5'-GGCTGTTGTCATACTTCTCATGG-3'. The specific experimental procedures were carried out in strict accordance with the kit instructions. Gene expression

was measured and normalized relative to the GAPDH level using the $2^{-\Delta\Delta Ct}$ method.

2.3. Data Collection and Processing. Expression matrices for 526 ccRCC samples and 72 normal ones were acquired from The Cancer Genome Atlas (TCGA, <https://portal.gdc.cancer.gov/repository>) database and filtered for samples with missing clinical and survival information, with gene expression as the mean value. Data about mutation data and copy number variation for ccRCC were also obtained from TCGA. Additionally, ninety-one primary renal cell cancer samples with complete prognostic and clinical information in the International Cancer Genome Consortium (ICGC, <https://dcc.icgc.org/>) were screened, and their expression profiles were downloaded.

2.4. Tumor Immunity. The relative proportions of the 22 immune cell compositions in the expression matrix were assessed using CIBERSORT, and $p < 0.05$ was used for subsequent comparisons. In addition, immune scores in tumor samples were calculated using the ESTIMATE algorithm, outputting scores for immune, stromal, and ESTIMATES.

2.5. Screening for SLC9A1 and mTOR-Related Genes and Gene Sets. The mTOR pathway-related genes were acquired from the official website of the Kyoto Encyclopedia of Genes and Genomes (KEGG, <https://www.genome.jp/kegg/>), and sample mTOR pathway scores were calculated using the ssGSEA algorithm. The correlation between gene sets and genes was calculated, respectively, on the basis of the Hmisc package rcorr function of the R language, and the correlated gene sets were screened by $|\text{cor}| > 0.25$ and $p < 0.001$.

2.6. Enrichment Analysis. Gene ontology (GO) enrichment analysis was conducted to explore the possible biological functions of the relevant genes in biological processes, cellular components, and molecular functions through the cluster Profiler package in R. A separate KEGG pathway enrichment analysis was performed to search for potential mechanisms.

2.7. Construction and Validation of the Prognostic Risk Model. Prognostic significance of genes was calculated by single and multifactor Cox analyses performed with the survival package. $p < 0.05$ was the selection criterion for screening for subsequent analyses. Candidate genes were subjected to lasso regression analysis using the R package glmnet for screening for prognosis-associated gene signatures, and models were constructed by 10-fold cross-validation.

$$\text{Risk score (patient)} = \sum_{i=1}^n \text{expression}_{\text{gene } i} \times \text{coefficient}_{\text{Gene } i} \quad (1)$$

The median risk score was defined with the R package survminer, and samples were classified according to the risk level. Kaplan–Meier (K–M) curves were drawn through the

R package time ROC to predict the prognostic classification efficiency of the risk score.

Module genes were extracted from published articles [21–23], and the c-index of these models was calculated and compared by the survcomp package.

2.8. Immunotherapy. The online software Tumor Immune Dysfunction and Exclusion (TIDE, <https://tide.dfci.harvard.edu/>) is used to assess the potential clinical effects of samples in immunotherapy.

2.9. Nomogram. The rms package was used along with the risk score and clinical characteristics to create nomogram that quantify the prognostic risk and likelihood of survival for patients at 1, 3, and 5 years. Moreover, usefulness of the model is also assessed by performing a decision curve analysis (DCA).

2.10. Statistical Analyses. With R software (3.6.1) and GraphPad Prism (9), statistical analyses were conducted, and the ggplot2 package was adopted for visualization. The correlation between gene expression and the pathway score was determined through Spearman correlation analysis and compared between the groups using the Wilcox test, $p < 0.05$.

3. Results

3.1. SLC9A1 Is Lowly Expressed in ccRCC. The overall flowchart is shown in Supplementary Figure 1. Comparison of TCGA expression profiles revealed lowly expressed SLC9A1 in ccRCC tumor tissues as compared with normal paracancerous tissues (Figure 1(a)). Moreover, qRT-PCR results revealed downregulated SLC9A1 in RCC cell strains as compared with normal kidney cell strains (Figure 1(b)). Next, we sorted out the mutation information of SLC9A1 through the SNV data of TCGA, and 2 samples had mutations in SLC9A1 gene, while 524 samples did not have mutations. As shown in Figure 1(c), gene expression in samples without SLC9A1 mutation was higher than that of the sample with SLC9A1 mutation, but there was no significant difference (maybe because of the too small sample size). Then, based on the CNV data of TCGA, the samples were divided into amplification, deletion, and diploid groups based on the CNV mutation of SLC9A1. We found that the samples without CNV mutation in SLC9A1 were significantly higher (Figure 1(d)).

3.2. Relationship between the Expression of SLC9A1 and Immunity. We found that some immune cells' scores expressed differently depending on the SLC9A1's expression

level (Figure 2(a)). The immune scores of the tumor samples showed that the highly expressed group of SLC9A1 had higher immune infiltration than the lowly expressed one (Figure 2(b)). Correlation analysis revealed a positive association between SLC9A1 expression and the immune score (Figure 2(c)). On the other hand, we also examined the correlation of the SLC9A1 expression with 22 types of immune cell scores. Among them, there was a positive correlation between SLC9A1 expression and score about Macrophages M0, T regulatory cells (Tregs), etc., and a negative correlation between it and cells, scores such as NK cells activated (Figure 2(d)). We extracted the genes of immune-related pathways, and the expression of some genes (e.g., IL6 and MMP9) in immune-related pathways also increased with the increased expression of SLC9A1 (Figure 2(e)).

3.3. Relationship between the SLC9A1 and mTOR Pathway and Gene Set Enrichment Analysis. The Spearman correlation analysis revealed positive association of SLC9A1 expression with the mTOR signaling pathway scores of the patients calculated by the ssGSEA method (Figure 3(a)). Further analysis screened 1502 genes positively associated with SLC9A1 expression, 1077 ones negatively associated with it, 3061 genes with positive association with the mTOR signaling pathway score, and 1611 ones with negative association with the score. By overlapping analysis, 564 genes were found to be associated with both SLC9A1 and mTOR (Figure 3(b)). Meanwhile, enrichment analysis of 564 related genes was conducted and the genes were found to be associated with actin filament-related biological processes, phagocytosis, and the cGMP-PKG signaling pathway (Figure 3(c)).

3.4. Construction and Validation of the ccRCC Prognostic Risk Model. We identified 39 genes mostly associated with the prognosis in both TCGA and ICGA datasets of ccRCC through univariate Cox regression analysis. Supplementary Table 1 presents the results of the one-way Cox analysis for the 564 genes in both TCGA and the ICGC datasets. Then, Lasso regression was performed to further reduce model genes for model optimization. The change trajectory of every independent variable was analyzed as shown in Figures 4(a) and 4(b). According to the results, with the gradual increase of lambda, the number of independent variable coefficients close to 0 also increased gradually. We used 10-fold cross-validation for model establishment. The confidence interval under every lambda was analyzed, and when lambda = 0.0344, the model is optimal. For this reason, we chose eleven genes with lambda = 0.0344 as the target genes. The risk score was calculated using the following formula:

$$\begin{aligned} \text{Risk score} = & 0.158 * \text{COL6A2} - 0.218 * \text{EXTL3} + 0.357 * \text{HEATR6} - 0.276 * \text{HSPG2} - 0.015 * \text{MAML3} \\ & + 0.389 * \text{PPP1R18} + 0.316 * \text{RCC2} + 0.173 * \text{SEMA7A} + 0.022 * \text{SERPINH1} - 0.484 * \text{TLN1} + 0.177 * \text{TM9SF4}. \end{aligned} \quad (2)$$

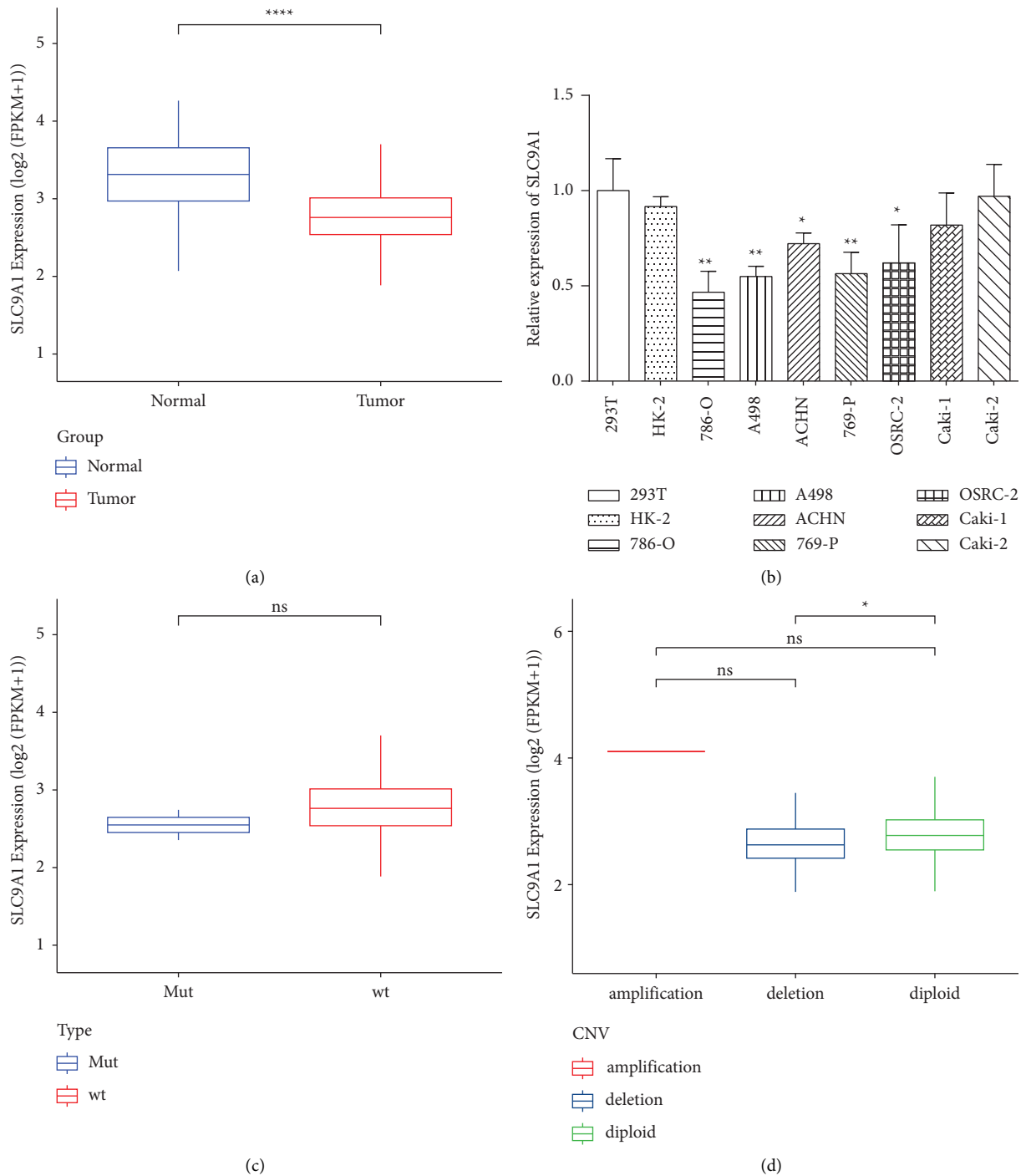


FIGURE 1: SLC9A1 is lowly expressed in ccRCC samples. (a) Expression of SLC9A1 in ccRCC cancer tissues and normal tissues in TCGA database. (b) qRT-PCR analysis of SLC9A1 in RCC cells vs. human normal renal cells (293T and HK-2). (c) Comparison of SLC9A1 expression between samples with or without SNV mutation. (d) Comparison of SLC9A1 expression between samples with or without CNV mutation. Note: SNV: single nucleotide variants; CNV: copy number variation. * $p < 0.05$, ** $p < 0.01$, *** $p < 0.001$, and **** $p < 0.0001$.

The expression of these 11 genes in cancer and normal paracancerous tissues is described in detail in Supplementary Figure 2. Next, we used TCGA dataset as the training dataset and calculated the risk score of every sample through the expression of 11 genes. The ROC curve assisted in evaluating the accuracy of OS estimates derived from the prognostic risk model. The classification efficiency of

1–5 year prognosis prediction was analyzed, and the area under curve (AUC) in 1–5 years reached above 0.7. In addition, the patients were assigned to a high- or low- risk group in the light of the mean value of the risk score. The K–M survival curve showed a notably worse overall survival (OS) in the high-risk group than that in the other group (Figures 4(c) and 4(d)). The same method was used to

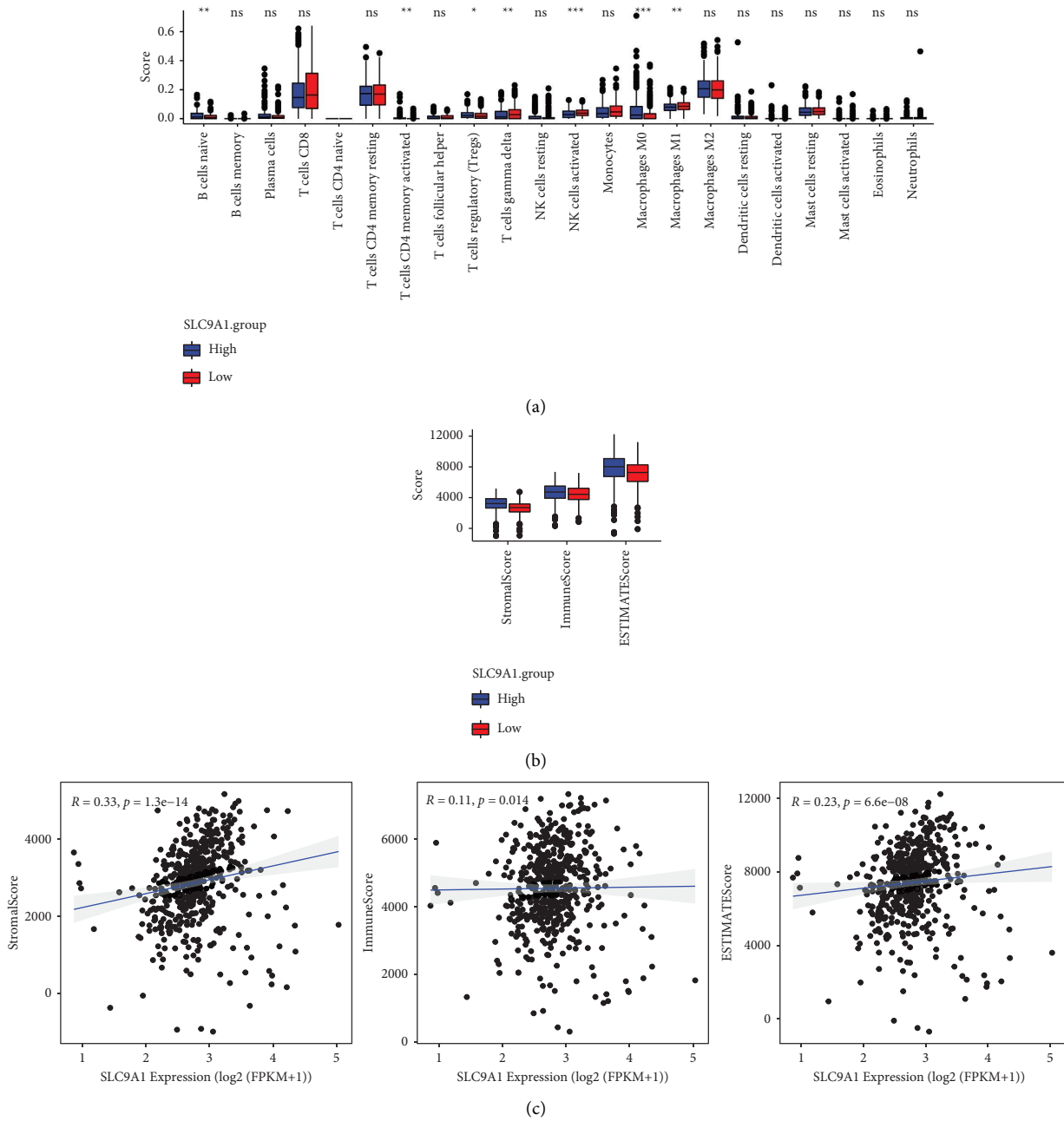


FIGURE 2: Continued.

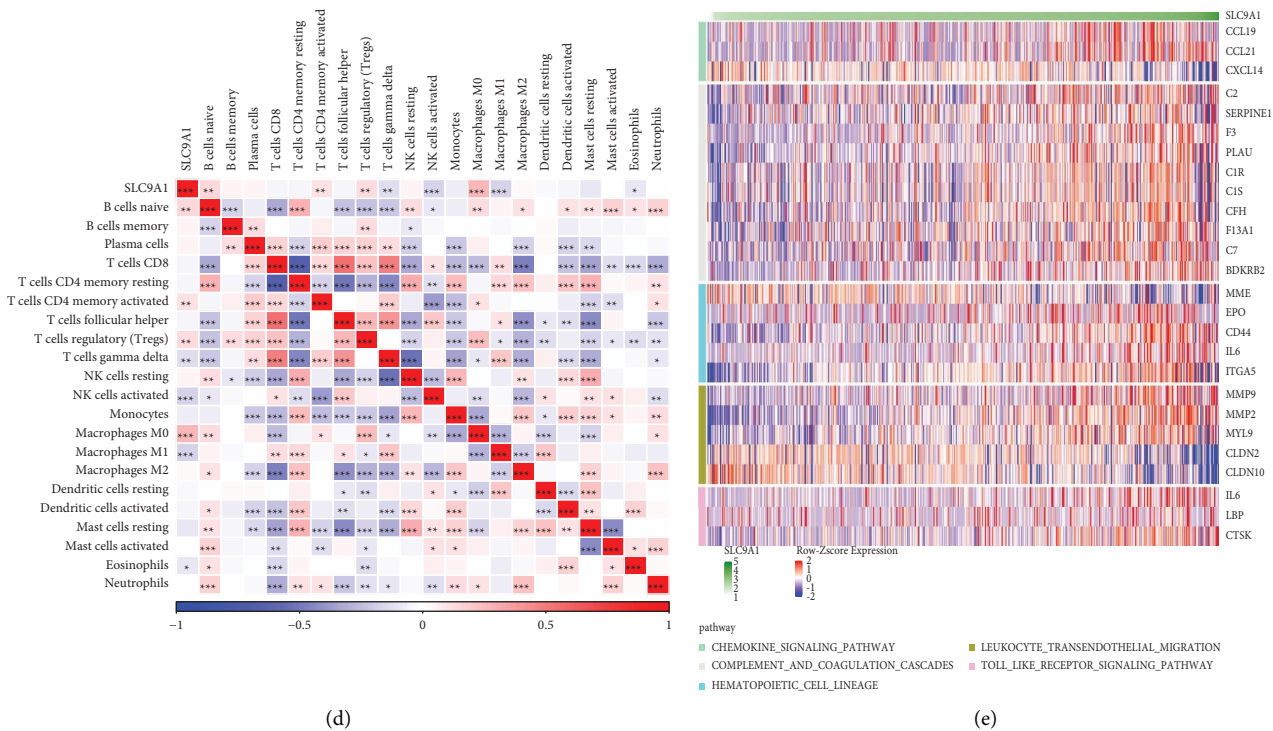


FIGURE 2: Expression of SLC9A1 correlates with the immune score and promotes immune cell infiltration. (a) Comparison of 22 types of immune cell scores with high and low expression of SLC9A1. (b) Comparison of immune cell infiltration between high and low expression of SLC9A1. (c) Correlation between the expression of SLC9A1 and the immune score. (d) Correlation between the expression of SLC9A1 and 22 immune cell scores. (e) A heatmap of the correlation between SLC9A1 and the expression of immune-related pathway genes. * $p < 0.05$, ** $p < 0.01$, and *** $p < 0.001$.

validate the ICGC dataset, and the similar results were observed (Figures 4(e) and 4(f)). Compared with the previous studies, our model is superior as shown in Supplementary Figure 3.

3.5. Association of the Prognostic Risk Model with Clinicopathological Characteristics. The differences in risk scores were compared for different clinicopathological characteristics, as shown in Figures 5(a)–5(f). The higher risk scores were significantly associated with higher TNM, histological grade, and advanced clinical staging. The risk score increases with T, M, and N stage, clinical stage, and histopathological grade.

3.6. Relationship between the Prognostic Risk Model and Immune Infiltration. We calculated scores for TCGA cohort samples at different risk levels in terms of 22 immune cells (Figure 6(a)), and the higher risk group had higher immune cell scores in some cells including CD8 T cells. Additionally, we also found higher immune scores in the high-risk group (Figure 6(b)). Immune checkpoint inhibitor therapy has gradually become the dominant method of systemic ccRCC treatment options [6]. Hence, the immune checkpoint genes in the high- and low-risk groups were analyzed, and the result showed significant differences in some immune checkpoint genes (Figure 6(c)). Next, as shown in Figure 6(d), the high-risk group got a higher TIDE score

than the low-risk group, which indicated that the high-risk group was more likely to have immune escape and less likely to benefit from immunotherapy.

3.7. Establishment and Validation of a Nomogram for Prediction of OS. Univariate and multivariate Cox regression analyses of the risk score and clinicopathological characteristics revealed that M stage, age, and the risk score were significant prognostic factors (Figures 7(a) and 7(b)). For quantifying the risk assessment and survival probability of ccRCC patients, we combined the risk score with other clinicopathological features to establish a nomogram (Figure 7(c)). Moreover, the results suggest that the risk score had the strongest influence on survival prediction. Furthermore, the calibration curve was adopted to evaluate the prediction accuracy of the model. It can be observed that the predicted calibration curves of the three calibration points at 1, 3, and 5 years were nearly coincident with the standard curve, which suggests the good performance of the nomogram (Figure 7(d)). From the results of decision curve analysis (DCA), the risk score and nomogram provided notably higher benefits than the extreme curves. In contrast to other clinicopathological characteristics, both the nomogram and the risk score exhibited the most powerful survival prediction ability (Figures 7(e) and 7(f)). These data demonstrate that our prognostic risk model is reliable and effective at predicting the prognosis of ccRCC patients.

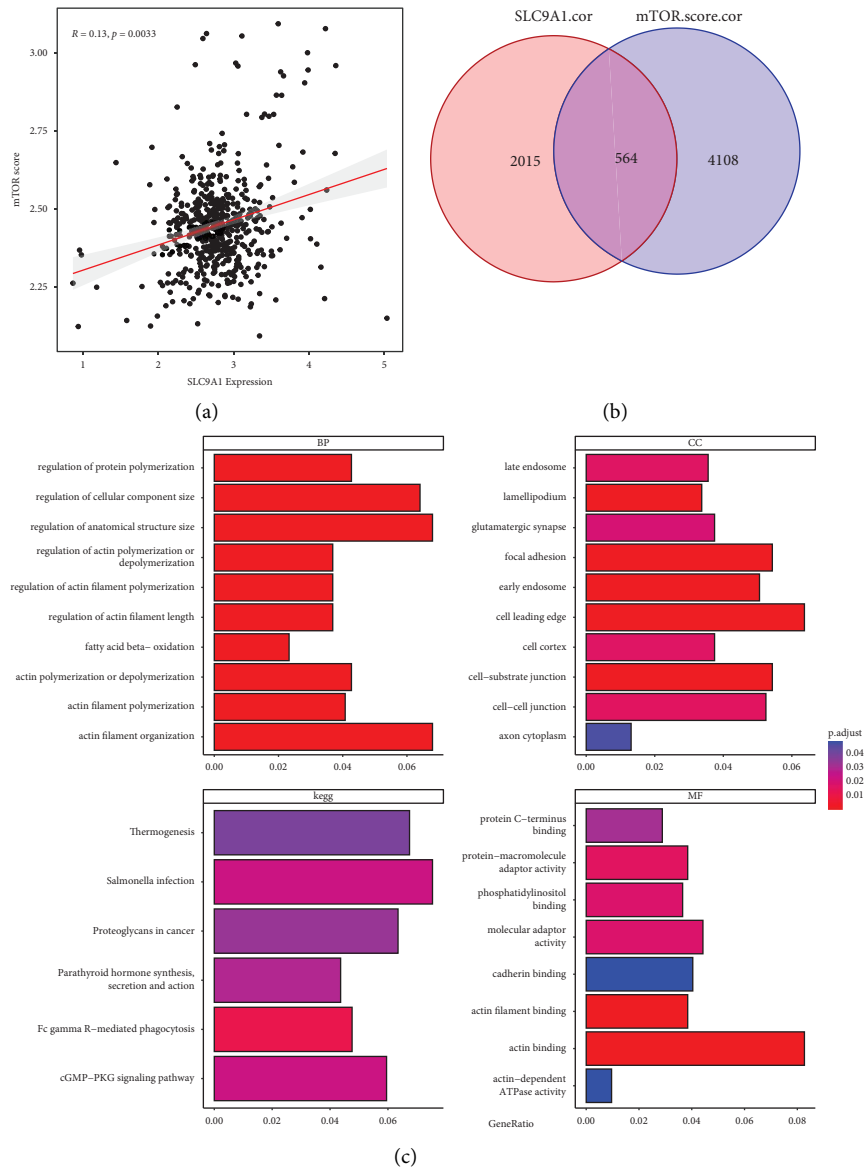
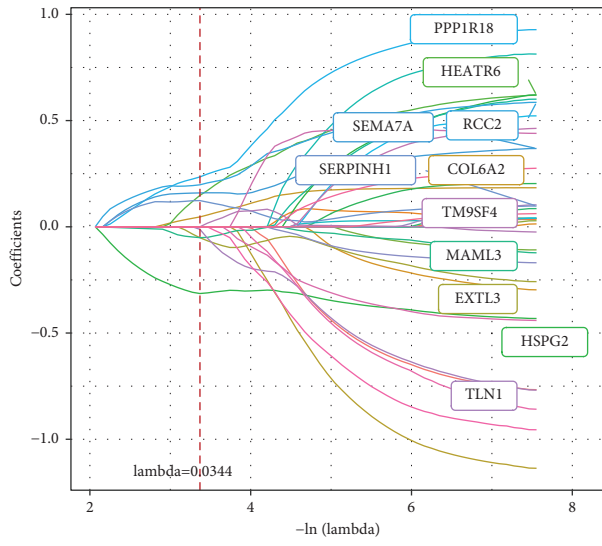


FIGURE 3: The expression of SLC9A1 combined with the expression of the mTOR signal pathway score. (a) Scatter plot of correlation between the expression of SLC9A1 and the mTOR signaling pathway score. (b) The Venn diagram shows 564 genes from both TCGA and ICGC gene sets. (c) Go and KEGG enrichment analysis of the 564 genes from both TCGA and ICGC gene sets. Note: GO: gene ontology; BP: biological process; CC: cellular components; MF: molecular functions.

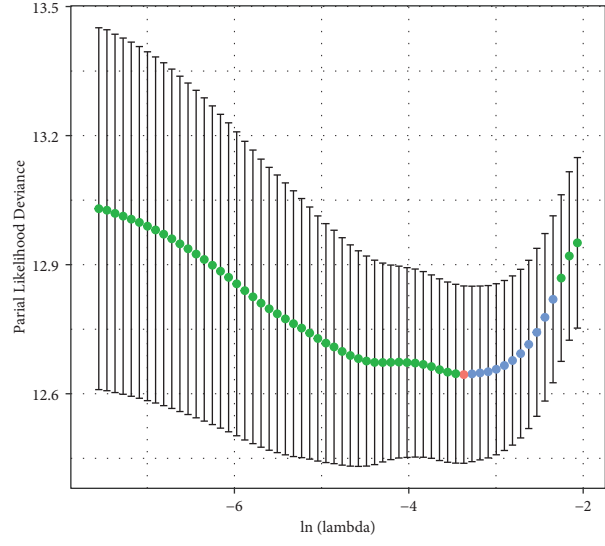
4. Discussion

SLC9A1 expression and potential function are becoming increasingly important in various cancers. For instance, tumor tissues showed significantly higher SLC9A1 expression than normal tissues in HCC and revealed that SLC9A1 expression can serve as a crucial prognostic factor for immunotherapy against HCC [24]. By contrast, as a novel prognostic biomarker in colorectal cancer, a lower level of SLC9A1 mRNA expression was observed [25]. According to analysis of TCGA data and qRT-PCR analysis in this study, SLC9A1 was downregulated in ccRCC. Prior research has shown that cell proliferation, motility, survival, and metabolism are all under control by the mTOR

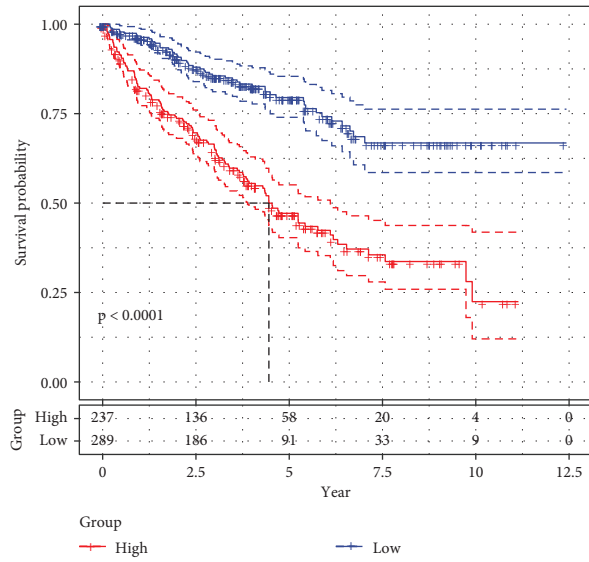
signaling pathway, and SLC9A1 may contribute to mTOR's tumor-promoting effects [17, 26, 27]. The mTOR inhibitors have been approved as a therapeutic option for metastatic ccRCC [28]. Given this, this relationship between SLC9A1 and the mTOR pathway in ccRCC is worth investigating. By analyzing genes related to prognosis step by step using Cox regression, Lasso regression, K-M survival analysis, and multi-cox regression, we constructed a prognosis gene panel with eleven genes having a prognostic risk score model (including COL6A2, EXTL3, HEATR6, HSPG2, MAML3, PPP1R18, RCC2, SEMA7A, SERPINH1, TLN1, and TM9SF4). Additionally, the prognostic risk model was used to determine the risk scores for TCGA cohort and ICGC cohort patients, and a high- and low-risk subgroup



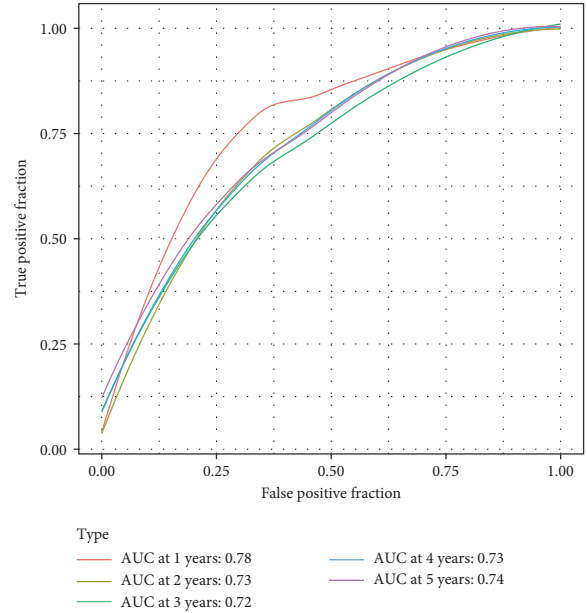
(a)



(b)



(c)



(d)

FIGURE 4: Continued.

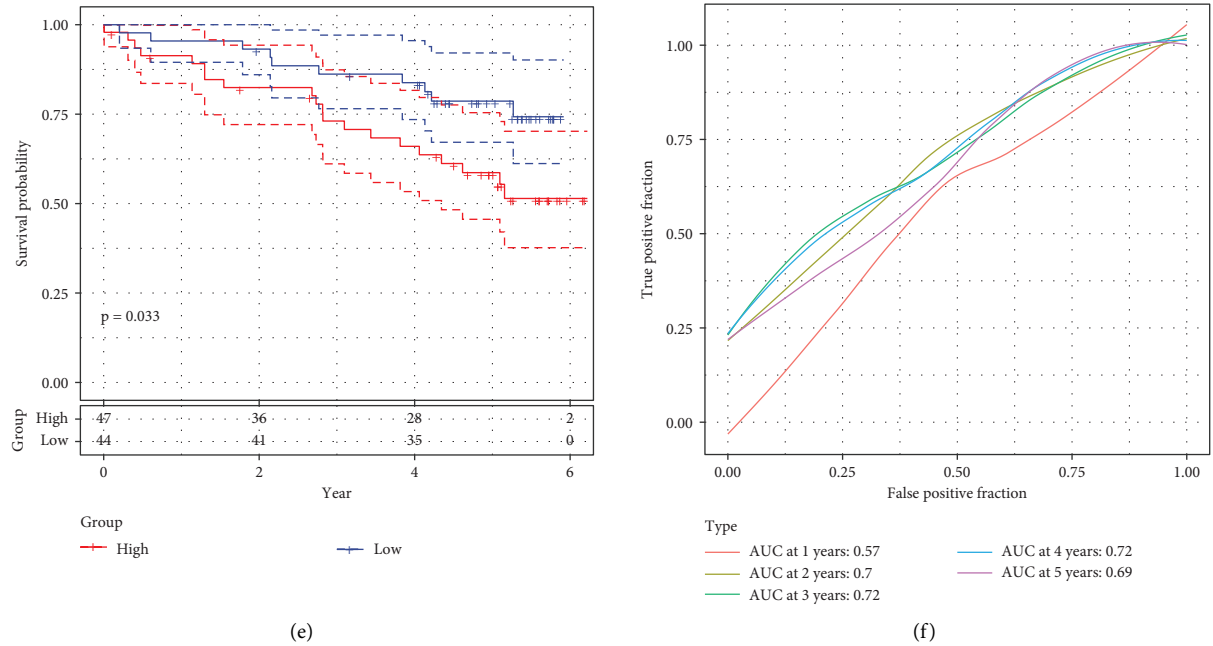


FIGURE 4: Construction of the prognostic risk model in TCGA cohort and ICGC cohort. (a) The trajectory of each gene coefficient with lambda. (b) 10-fold cross-validation was used to find the best values for the penalty parameter. (c) The Kaplan–Meier (K–M) survival curve showed patients in the high- and low-risk group in TCGA dataset. (d) The prognostic signature’s ROC curve at 1, 2, 3, 4, and 5 years in TCGA dataset. (e) The K–M survival curve showed that patients in the high- and low-risk group in the ICGC dataset. (f) The prognostic signature’s ROC curve at 1, 2, 3, 4, and 5 years in the ICGC dataset.

for ccRCC patients was identified. Based on the K–M survival analysis and ROC curve, the eleven genes exhibited effective and reliable predictive abilities in the training set, with a significantly shorter OS in high-risk patients than that in low-risk ones. Furthermore, the association of the prognostic risk model with clinicopathological characteristics was verified. The results revealed association of the risk score with clinicopathological characteristics. The risk score and other clinicopathological characteristics were combined to establish a nomogram, and the calibration curve showed the effectiveness of the nomogram. We also used DCA to evaluate the models, and the results showed that the constructed prognostic risk model is strong and generalizable.

In liver HCCs, SLC9A1 was strongly related with immune cell infiltration [24]. SLC9A1 blockade boosts immunity to glioma tumors by restoring oxidative stress in myeloid cells [29]. During this research, we found that the highly expressed group of SLC9A1 had higher immune infiltration in tumor samples and was closely associated with multiple immune cell scores. Alternatively, SLC9A1 participated in partial immune-related signaling pathways. Immune cell infiltrating tumors play an important prognostic role [30]. Therefore, we explored the immune signatures of the prognostic risk model. According to the results, the high-risk group presented a stronger immune cell infiltration and got a higher TIDE score, which indicated that the group was less likely to benefit from immunotherapy. These results may spark novel ideas for research, diagnosis, and treatment of ccRCC.

Eleven genes, COL6A2, EXTL3, HEATR6, HSPG2, MAML3, PPP1R18, RCC2, SEMA7A, SERPINH1, TLN1, and TM9SF4, were selected as important prognostic markers. COL6A2 is a member of the Collagen VI family and widely expressed in various cancers and promotes cancer progression. COL6A2 was also positively associated with an increased risk in the model of the current study (coefficient > 0). Zhong et al. found an up-regulation of COL6A2, which could be a factor in poor prognosis in metastatic ccRCC [31]. Exostosin-like glycosyltransferase 3 (EXTL3), belonging to the EXT family, takes a crucial part in predicting the prognosis of various cancers and immune deficiencies [32], but its role in ccRCC remains unknown. HEAT repeat containing 6 (HEATR6) is part of a highly expressed breast cancer amplicon. Prior research indicated that endometrial tumors from African-American women express elevated levels of HEATR6 [33]. There are few research studies of HEATR6 in ccRCC. A recent study showed that heparan sulfate proteoglycan 2 (HSPG2) participates in tumor and stromal cell binding to the extracellular matrix of ccRCC, and HSPG2 showed the strongest binding to FN1, COL6, and COL12 in all cells [34]. Zhang et al. confirmed that silencing MAML3 suppresses the proliferation of gastric cancer by acting as a transcriptional coactivator in the Notch signaling pathway [35]. Genetic alterations in MAML3 and the Notch pathway in which it resides also appear to give a better prognosis for patients with ccRCC [36]. As a biomarker for immunotherapy, protein phosphatase 1 regulatory subunit 18 (PPP1R18) serves as an oncogenic role in ccRCC and was significantly related with immunity [37]. The

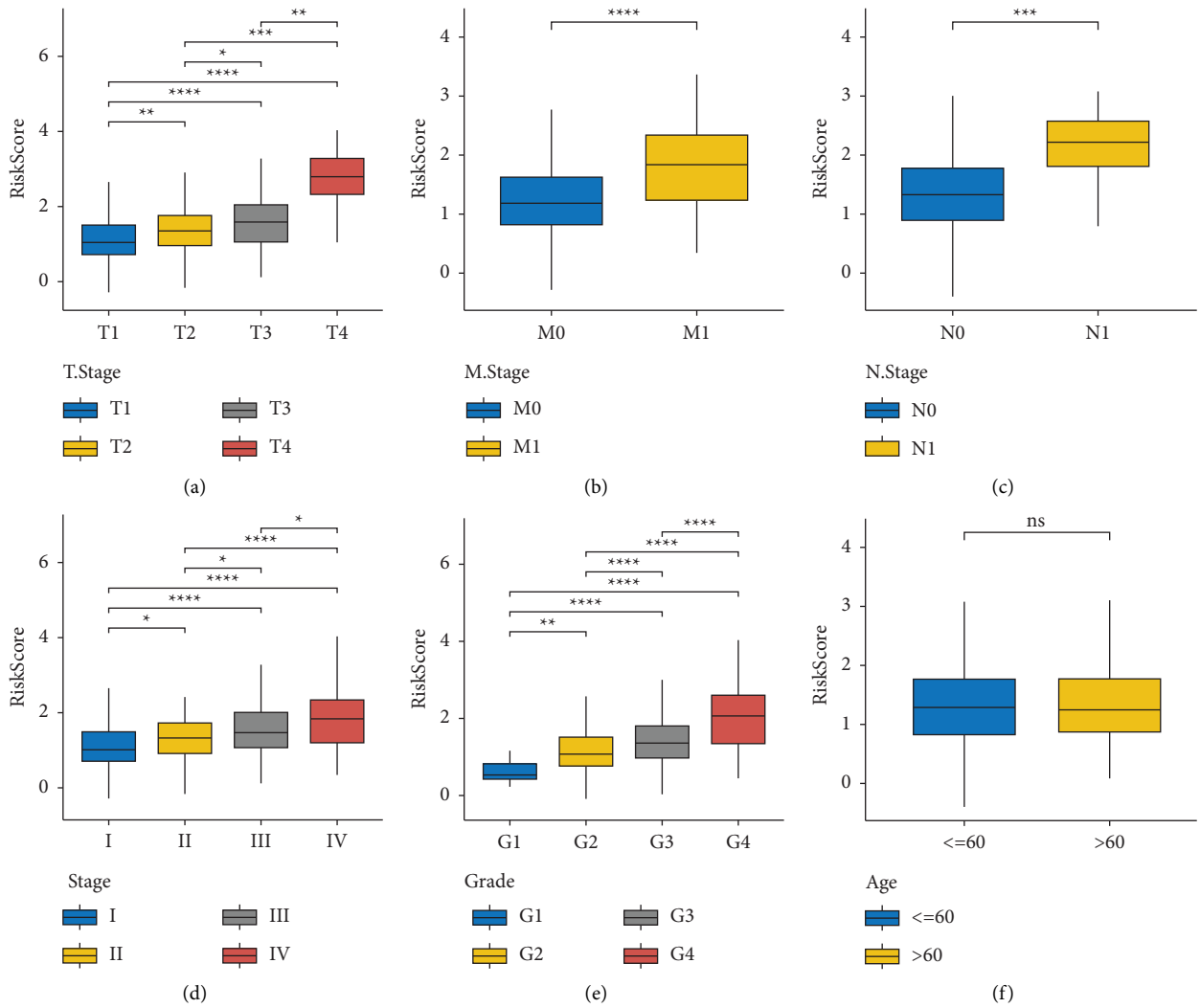


FIGURE 5: Comparison of the risk score for different clinicopathological characteristics. (a) T stage. (b) M stage. (c) N stage. (d) Clinical stage. (e) Histopathological grade. (f) Age. * $p < 0.05$, ** $p < 0.01$, *** $p < 0.001$, and **** $p < 0.0001$.

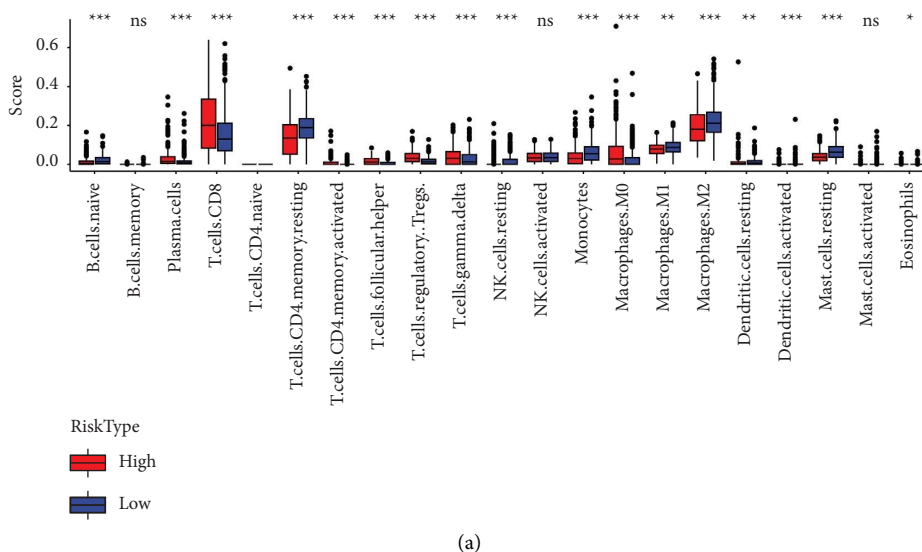


FIGURE 6: Continued.

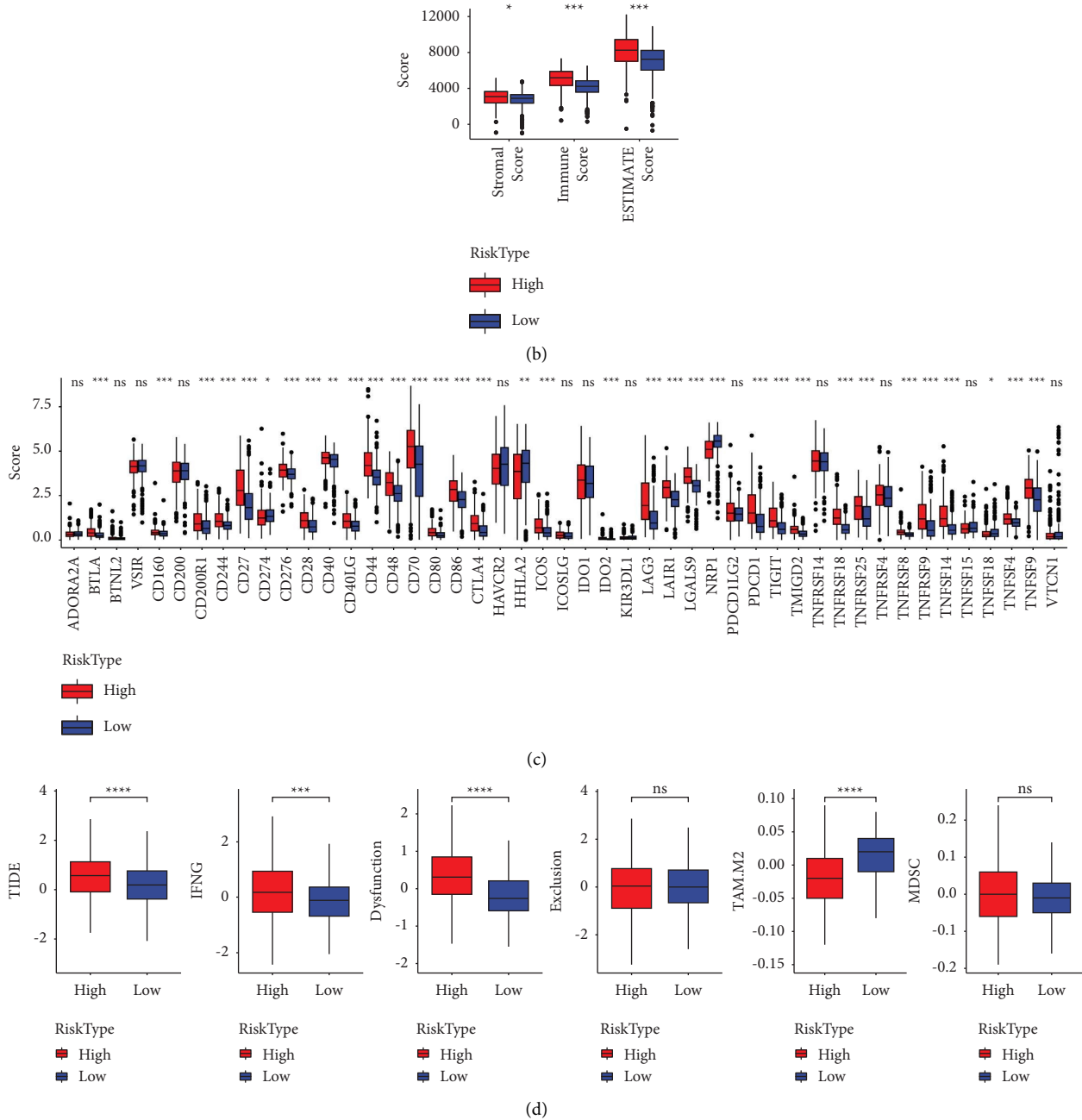


FIGURE 6: Comparison of immunological characteristics of different risk groups and differences of 22 immune cell scores (a), stromal, immune, and ESTIMATE scores (b) of the high- and low-risk groups in TCGA cohort. (c) Immune checkpoint genes differentially expressed in different risk groups in TCGA cohort. (d) The TIDE analysis results of different risk groups in TCGA cohort. * $p < 0.05$, ** $p < 0.01$, *** $p < 0.001$, and **** $p < 0.0001$.

literature confirmed that chromosome condensation 2 (RCC2) was an oncogene and took a crucial part in promoting the proliferation of lung adenocarcinoma, esophageal squamous cell carcinoma, and acute myeloid leukemia [38]. The GPI-anchored semaphorin 7A (SEMA7A) affects inflammatory diseases, and Wang et al. found association of a high SEMA7A level with poor outcomes in ccRCC [39]. Serpin peptidase inhibitor clade H member 1 (SERPINH1), also known as HSP47, belongs to the serpin superfamily. The level of SERPINH1 is significantly elevated at the four TNM

stages of ccRCC tissues and strongly correlates with unfavorable clinical outcomes [40]. The talin 1 (TLN1) receptor mediates cell adhesion, regulates integrin signaling, and promotes metastasis in various cancers, such as prostate, colon, and oral cancer [41]. According to Guazzi et al., transmembrane 9 superfamily 4 (TM9SF4) is a highly specific cancer biomarker that can be adopted to detect and stage gastrointestinal cancers [42], and its role in ccRCC remains unclear. The results of the present study show that these 11 genes are related with the prognosis of ccRCC

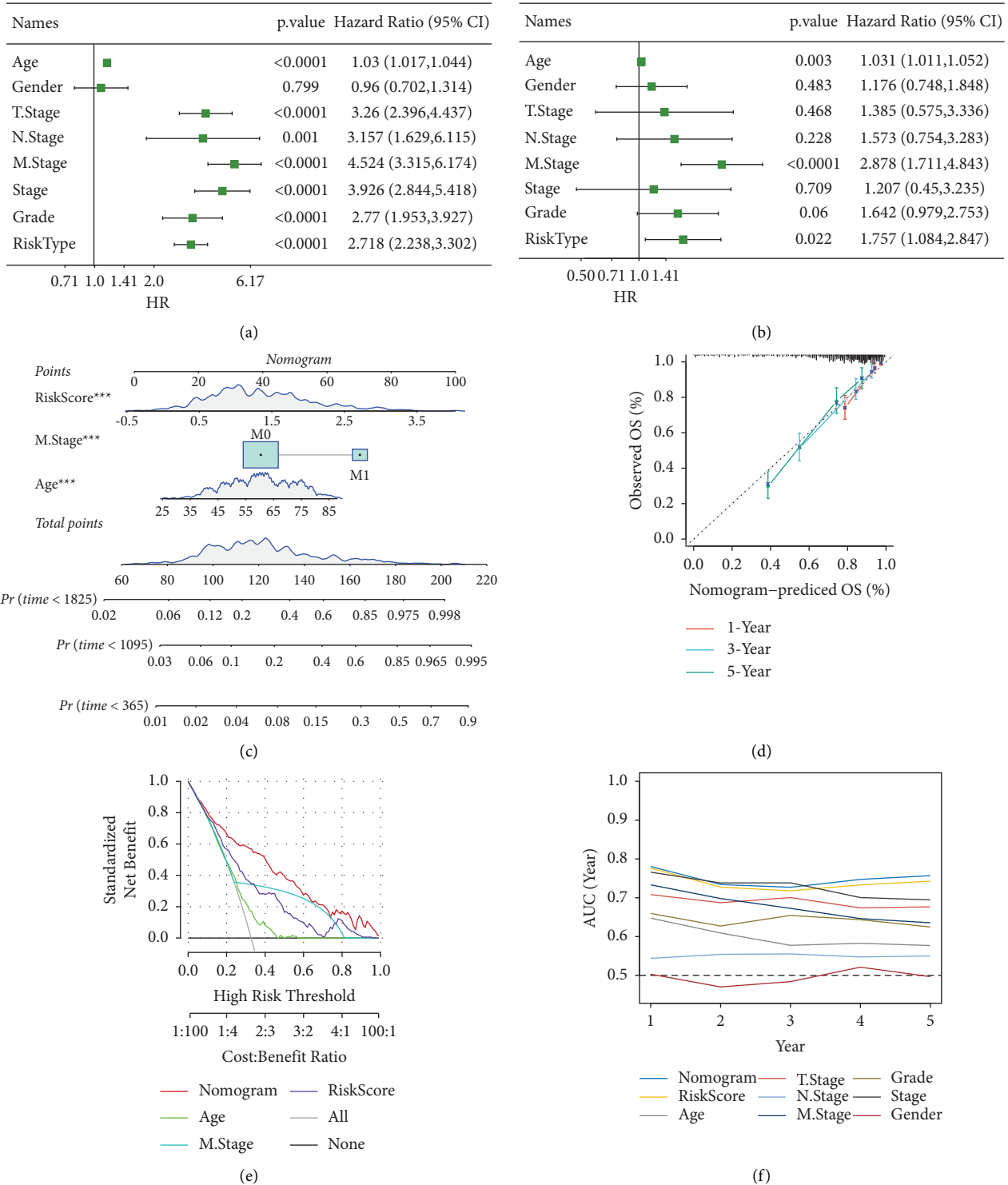


FIGURE 7: Construction of a nomogram and verification that the risk score has a powerful survival prediction ability. Univariate (a) and multivariate (b) Cox regression analysis of the risk score and clinicopathological characteristics in ccRCC patients. (c) The development of a nomogram based on the risk score and clinicopathological characteristics. (d) The calibration curve of the nomogram in 1, 3, and 5 years. (e) Decision curve of the nomogram. (f) Compared with other clinicopathological features, the nomogram and the risk score exhibited the more powerful capacity for survival prediction.

patients, but the exact mechanism still involves a huge network of gene regulation, which needs further exploration.

Because of the sample specificity of ccRCC, the dataset that could be selected for this study was small. Further validation of how SLC9A1 mediates mTOR signaling in ccRCC through ex vivo experimental data will be the direction of our subsequent studies. We also expect more scholars to explore this direction and more relevant datasets in the future for early validation of this risk model in a clinical cohort.

5. Conclusion

In summary, we have constructed a risk model consisting of 11 genes based on SLC9A1 and mTOR signaling-related genes in ccRCC, which has great potential for prognostic assessment in ccRCC. The model can guide clinical immunotherapy to accurately identify high-risk patients for early clinical intervention.

Data Availability

The bioinformatic data were used to support this study and are available at TCGA and GEO databases. These prior datasets are cited at relevant places within the text as references.

Conflicts of Interest

The authors declare that they have no conflicts of interest.

Acknowledgments

This study was supported by the National Natural Science Foundation of China (Grant no. 81902601).

Supplementary Materials

Supplementary Figure 1: the overall flowchart for this work. Supplementary Figure 2: expression of 11 genes in cancer and adjacent tissues. Supplementary Figure 3: comparison with models in previously published studies. Supplementary Table 1: results of the univariate COX analysis of 564 genes in TCGA dataset and the ICGC dataset. (*Supplementary Materials*)

References

- [1] D. J. Clark, S. M. Dhanasekaran, F. Petralia et al., "Integrated proteogenomic characterization of clear cell renal cell carcinoma," *Cell*, vol. 180, no. 1, p. 207, 2020.
- [2] Y. Wang, R. Cong, S. Liu, B. Zhu, X. Wang, and Q. Xing, "Decreased expression of METTL14 predicts poor prognosis and construction of a prognostic signature for clear cell renal cell carcinoma," *Cancer Cell International*, vol. 21, no. 1, p. 46, 2021.
- [3] H. Moch, A. L. Cubilla, P. A. Humphrey, V. E. Reuter, and T. M. Ulbright, "The 2016 WHO classification of tumours of the urinary system and male genital organs—Part A: renal, penile, and testicular tumours," *European Urology*, vol. 70, no. 1, pp. 93–105, 2016.
- [4] C. Zhu, Z. Song, Z. Chen et al., "MicroRNA-4735-3p facilitates ferroptosis in clear cell renal cell carcinoma by targeting SLC40A1," *Analytical Cellular Pathology*, vol. 2022, Article ID 4213401, 12 pages, 2022.
- [5] C. M. Diaz-Montero, B. I. Rini, and J. H. Finke, "The immunology of renal cell carcinoma," *Nature Reviews Nephrology*, vol. 16, no. 12, pp. 721–735, 2020.
- [6] Y. F. Liu, Z. C. Zhang, S. Y. Wang et al., "Immune checkpoint inhibitor-based therapy for advanced clear cell renal cell carcinoma: a narrative review," *International Immunopharmacology*, vol. 110, Article ID 108900, 2022.
- [7] W. Xu, M. B. Atkins, and D. F. McDermott, "Checkpoint inhibitor immunotherapy in kidney cancer," *Nature Reviews Urology*, vol. 17, no. 3, pp. 137–150, 2020.
- [8] H. Sung, J. Ferlay, R. L. Siegel et al., "Global cancer statistics 2020: GLOBOCAN estimates of incidence and mortality worldwide for 36 cancers in 185 countries," *CA: A Cancer Journal for Clinicians*, vol. 71, no. 3, pp. 209–249, 2021.
- [9] A. Deleuze, J. Saout, F. Dugay et al., "Immunotherapy in renal cell carcinoma: the future is now," *International Journal of Molecular Sciences*, vol. 21, no. 7, p. 2532, 2020.
- [10] P. C. Barata and B. I. Rini, "Treatment of renal cell carcinoma: current status and future directions," *CA: A Cancer Journal for Clinicians*, vol. 67, no. 6, pp. 507–524, 2017.
- [11] T. K. Choueiri, S. Halabi, B. L. Sanford et al., "Cabozantinib versus sunitinib as initial targeted therapy for patients with metastatic renal cell carcinoma of poor or intermediate risk: the alliance A031203 CABOSUN trial," *Journal of Clinical Oncology*, vol. 35, no. 6, pp. 591–597, 2017.
- [12] Mammalian Gene Collection Mgc Program Team, E. A. Feingold, L. H. Grouse, J. G. Derge, R. D. Klausner, and F. S. Collins, "Generation and initial analysis of more than 15,000 full-length human and mouse cDNA sequences," *Proceedings of the National Academy of Sciences of the United States of America*, vol. 99, no. 26, pp. 16899–16903, 2002.
- [13] R. Xie, H. Wang, H. Jin, G. Wen, B. Tuo, and J. Xu, "NHE1 is upregulated in gastric cancer and regulates gastric cancer cell proliferation, migration and invasion," *Oncology Reports*, vol. 37, no. 3, pp. 1451–1460, 2017.
- [14] M. Mazzocchi, G. Di Giusto, M. Porta et al., "Na⁺/H⁺ exchanger isoform 1 activity in AQP2-expressing cells can be either proliferative or anti-proliferative depending on extracellular pH," *Journal of Physiology & Biochemistry*, vol. 76, no. 1, pp. 37–48, 2020.
- [15] M. J. Hovde, D. E. Bolland, A. Armand et al., "Sodium hydrogen exchanger (NHE1) palmitoylation and potential functional regulation," *Life Sciences*, vol. 288, Article ID 120142, 2022.
- [16] P. G. Valles, V. Bocanegra, A. Gil Lorenzo, and V. V. Costantino, "Physiological Functions and Regulation of the Na⁺/H⁺Exchanger [NHE1] in Renal Tubule Epithelial Cells," *Kidney & Blood Pressure Research*, vol. 40, no. 5, pp. 452–466, 2015.
- [17] D. W. Good, T. George, and B. A. Watts, "Nerve growth factor inhibits Na⁺/H⁺ exchange and HCO₃⁻ absorption through parallel phosphatidylinositol 3-Kinase-mTOR and ERK pathways in thick ascending limb," *Journal of Biological Chemistry*, vol. 283, no. 39, pp. 26602–26611, 2008.
- [18] C. Sanhueza, J. Araos, L. Naranjo et al., "NHE1 promote cell proliferation in ovarian cancer: a role of hypoxia-inducible factors.: IGCS-0038 06. Ovarian cancer[.]," *International Journal of Gynecological Cancer*, vol. 25, no. Suppl 1, pp. 55-56, 2015.

- [19] X. Guan, L. Luo, G. Begum et al., "Elevated Na/H exchanger 1 (SLC9A1) emerges as a marker for tumorigenesis and prognosis in gliomas," *Journal of Experimental & Clinical Cancer Research*, vol. 37, no. 1, p. 255, 2018.
- [20] X. Li and L. Fliegel, "Permissive role of Na⁺/H⁺ exchanger isoform 1 in migration and invasion of triple-negative basal-like breast cancer cells," *Molecular and Cellular Biochemistry*, vol. 477, no. 4, pp. 1207–1216, 2022.
- [21] K. Li, Y. Li, Y. Lyu et al., "Development of a phagocytosis-dependent gene signature to predict prognosis and response to checkpoint inhibition in clear-cell renal cell carcinoma," *Frontiers in Immunology*, vol. 13, Article ID 853088, 2022.
- [22] Z. Li, G. Du, R. Zhao et al., "Identification and validation of a hypoxia-related prognostic signature in clear cell renal cell carcinoma patients," *Medicine (Baltimore)*, vol. 100, no. 39, Article ID e27374, 2021.
- [23] Y. Chen, Y. Liang, Y. Chen, S. Ouyang, K. Liu, and W. Yin, "Identification of prognostic metabolism-related genes in clear cell renal cell carcinoma," *JAMA Oncology*, vol. 2021, Article ID 2042114, 13 pages, 2021.
- [24] Y. T. Zhou, H. Chen, M. Ai et al., "Type-1 Na⁺/H⁺ exchanger is a prognostic factor and associate with immune infiltration in liver hepatocellular carcinoma," *Life Sciences*, vol. 278, Article ID 119613, 2021.
- [25] X. Zhou, M. Jiang, Z. Liu et al., "Na⁺/H⁺-Exchanger family as novel prognostic biomarkers in colorectal cancer," *JAMA Oncology*, vol. 2021, Article ID 3241351, 22 pages, 2021.
- [26] G. Y. Liu and D. M. Sabatini, "mTOR at the nexus of nutrition, growth, ageing and disease," *Nature Reviews Molecular Cell Biology*, vol. 21, no. 4, pp. 183–203, 2020.
- [27] D. Mossmann, S. Park, and M. N. Hall, "mTOR signalling and cellular metabolism are mutual determinants in cancer," *Nature Reviews Cancer*, vol. 18, no. 12, pp. 744–757, 2018.
- [28] H. Guo, P. German, S. Bai et al., "The PI3K/AKT pathway and renal cell carcinoma," *Journal of Genetics and Genomics*, vol. 42, no. 7, pp. 343–353, 2015.
- [29] M. N. Hasan, L. Luo, D. Ding et al., "Blocking NHE1 stimulates glioma tumor immunity by restoring OXPHOS function of myeloid cells," *Theranostics*, vol. 11, no. 3, pp. 1295–1309, 2021.
- [30] G. Wieers, N. Demotte, D. Godelaine, and P. Van der Bruggen, "Immune suppression in tumors as a surmountable obstacle to clinical efficacy of cancer vaccines," *Cancers*, vol. 3, no. 3, pp. 2904–2954, 2011.
- [31] T. Zhong, Z. Jiang, X. Wang et al., "Key genes associated with prognosis and metastasis of clear cell renal cell carcinoma," *PeerJ*, vol. 10, Article ID e12493, 2022.
- [32] P. Chang, S. Chen, X. Chang, J. Zhu, Q. Tang, and L. Ma, "EXTL3 could serve as a potential biomarker of prognosis and immunotherapy for prostate cancer and its potential mechanisms," *European Journal of Medical Research*, vol. 27, no. 1, p. 115, 2022.
- [33] M. D. Kessler, N. W. Bateman, T. P. Conrads, G. L. Maxwell, J. C. Dunning Hotopp, and T. D. O'Connor, "Ancestral characterization of 1018 cancer cell lines highlights disparities and reveals gene expression and mutational differences," *Cancer*, vol. 125, no. 12, pp. 2076–2088, 2019.
- [34] K. H. Bond, T. Chiba, K. P. H. Wynne et al., "The extracellular matrix environment of clear cell renal cell carcinoma determines cancer associated fibroblast growth," *Cancers*, vol. 13, no. 23, p. 5873, 2021.
- [35] Q. Zha, X. Wu, J. Zhang et al., "Hsa_circ_0007967 promotes gastric cancer proliferation through the miR-411-5p/MAML3 axis," *Cell Death & Disease*, vol. 8, no. 1, p. 144, 2022.
- [36] C. Feng, Z. Xiong, H. Jiang, Q. Ding, Z. Fang, and W. Hui, "Genetic alteration in notch pathway is associated with better prognosis in renal cell carcinoma," *BioFactors*, vol. 42, no. 1, pp. 41–48, 2016.
- [37] Y. Wang, S. Liu, Y. Chen, B. Zhu, and Q. Xing, "Survival prognosis, tumor immune landscape, and immune responses of PPP1R18 in kidney renal clear cell carcinoma and its potentially double mechanisms," *World Journal of Oncology*, vol. 13, no. 1, pp. 27–37, 2022.
- [38] N. Zhang, Y. Shen, H. Li et al., "The m6A reader IGF2BP3 promotes acute myeloid leukemia progression by enhancing RCC2 stability," *Experimental and Molecular Medicine*, vol. 54, no. 2, pp. 194–205, 2022.
- [39] Y. Wang, C. Li, X. Qi et al., "A comprehensive prognostic analysis of tumor-related blood group antigens in pan-cancers suggests that SEMA7A as a novel biomarker in kidney renal clear cell carcinoma," *International Journal of Molecular Sciences*, vol. 23, no. 15, p. 8799, 2022.
- [40] Y. Qi, Y. Zhang, Z. Peng et al., "SERPINH1 overexpression in clear cell renal cell carcinoma: association with poor clinical outcome and its potential as a novel prognostic marker," *Journal of Cellular and Molecular Medicine*, vol. 22, no. 2, pp. 1224–1235, 2018.
- [41] Y. Zhang, L. Sun, H. Li et al., "Binding blockade between TLN1 and integrin beta1 represses triple-negative breast cancer," *Elife*, vol. 11, 2022.
- [42] P. Guazzi, D. Zocco, S. Isajevs et al., "TM9SF4 expression in tumor tissues: a novel diagnostic biomarker for gastrointestinal tumors," *Translational Cancer Research*, vol. 9, no. 11, pp. 6652–6659, 2020.